Human Molecular Genetics, 2010, Vol. 19, No. 5 **803–814**
doi:10.1093/hmg/ddp549
Advance Access published on December 9, 2009

Analysis of the *IGF2/H19* imprinting control region uncovers new genetic defects, including mutations of OCT-binding sequences, in patients with 11p15 fetal growth disorders

Julie Demars[1,†], Mansur Ennuri Shmela[1,†], Sylvie Rossignol[2], Jun Okabe[1], Irène Netchine[2], Salah Azzi[2], Sylvie Cabrol[2], Cédric Le Caignec[3,4], Albert David[3], Yves Le Bouc[2], Assam El-Osta[1] and Christine Gicquel[1,*]

[1]Epigenetics in Human Health and Disease, Baker IDI Heart and Diabetes Institute, Melbourne, 3004 VIC, Australia, [2]Laboratoire d'Explorations Fonctionnelles Endocriniennes, Unité mixte de recherche INSERM UMPC U938, APHP, Hopital Armand Trousseau, Paris 75012, France, [3]Service de Génétique Médicale, CHU, Nantes 44093, France and [4]INSERM, UMR915, Institut du thorax, Nantes 44035, France

Received August 17, 2009; Revised and Accepted December 7, 2009

The imprinted expression of the *IGF2* and *H19* genes is controlled by the imprinting control region 1 (ICR1) located at chromosome 11p15.5. This methylation-sensitive chromatin insulator works by binding the zinc-finger protein CTCF in a parent-specific manner. DNA methylation defects involving the ICR1 *H19/IGF2* domain result in two growth disorders with opposite phenotypes: an overgrowth disorder, the Beckwith–Wiedemann syndrome (maternal ICR1 gain of methylation in 10% of BWS cases) and a growth retardation disorder, the Silver–Russell syndrome (paternal ICR1 loss of methylation in 60% of SRS cases). Although a few deletions removing part of ICR1 have been described in some familial BWS cases, little information is available regarding the mechanism of ICR1 DNA methylation defects. We investigated the *CTCF* gene and the ICR1 domain in 21 BWS patients with ICR1 gain of methylation and 16 SRS patients with ICR1 loss of methylation. We identified four constitutional ICR1 genetic defects in BWS patients, including a familial case. Three of those defects are newly identified imprinting defects consisting of small deletions and a single mutation, which do not involve one of the CTCF binding sites. Moreover, two of those defects affect OCT-binding sequences which are suggested to maintain the unmethylated state of the maternal allele. A single-nucleotide variation was identified in a SRS patient. Our data extends the spectrum of constitutive genetic ICR1 abnormalities and suggests that extensive and accurate analysis of ICR1 is required for appropriate genetic counseling in BWS patients with ICR1 gain of methylation.

INTRODUCTION

Human chromosome 11p15.5 contains a cluster of imprinted genes that play a crucial role in the control of fetal growth (1–3). This cluster is organized in two neighboring imprinted domains, the *IGF2/H19* and the *KCNQ1* domains, each of them under the control of its own imprinting center, ICR1 and ICR2, respectively. Aberrant genomic imprinting of the 11p15 region has a pivotal role in both Beckwith–Wiedemann (BWS; MIM 130650) and Silver–Russell (SRS; MIM 180860) fetal growth disorders. BWS is characterized by pre-and/or post-natal overgrowth and other features including hemihyperplasia and an increased risk of tumors. SRS is characterized by severe pre- and post-natal growth retardation, dysmorphic facial features, feeding difficulties and body asymmetry. A variety of 11p15 molecular aberrations have been demonstrated

*To whom correspondence should be addressed at: Epigenetics in Human Health and Disease, Baker IDI Heart and Diabetes Institute, 75 Commercial Road, Melbourne, 3004 VIC, Australia. Tel: +61 385321310; Fax: +61 385321100; Email: christine.gicquel@bakeridi.edu.au
†The authors wish it to be known that, in their opinion, the first two authors should be regarded as joint First Authors.

in BWS and SRS (4–6). Epigenetic alterations account for ~60–70% of BWS and SRS cases. DNA methylation defects involving the ICR2 *KCNQ1* domain (loss of methylation) result in BWS (60% of cases), whereas DNA methylation defects involving the ICR1 *H19/IGF2* domain result in both BWS (gain of methylation, 10% of cases) and SRS (loss of methylation, 60% of cases) (4,5,7,8).

The reciprocal imprinting of the maternally expressed *H19* and the paternally expressed *IGF2* genes depends on the differentially methylated ICR1 upstream from the *H19* gene, which acts as an insulator. ICR1 is methylated exclusively on the paternal allele and is one of the rare ICRs that is marked in the male germ line (9). ICR1 binding of the zinc-finger CTCF protein mediates higher-order chromatin conformation, partitioning paternal and maternal *IGF2* alleles into active and inactive chromatin domains (10–12). CTCF binds the maternal unmethylated ICR1 resulting in a specific change in chromatin loop structure and prevents the *IGF2* gene promoter from interacting with enhancers downstream from the *H19* gene, resulting in transcriptional silencing of the maternal *IGF2* allele (10). On the paternal allele, DNA methylation prevents CTCF binding and is permissive for *IGF2* gene activation. CTCF is also required for normal pre-implantation development and maintenance of the unmethylated state of ICR1 on the maternal allele (13,14).

In a few familial BWS cases with a gain of methylation at ICR1, deletions within ICR1 have been reported; such deletions result in a BWS phenotype only if the deletion is maternally inherited (15–18). Subjects who inherited the microdeletion from the father do not display any phenotype and, more particularly, no SRS phenotype. Besides, Engel *et al*. (14) have showed that depletion in CpG residues in *H19* DMD (mouse ICR1) results in a fetal growth retardation phenotype when paternally inherited. Moreover, the affected mice display abnormal ICR1 DNA methylation similar to SRS patients. ICR1 CTCF binding sites have been investigated for mutation in a few sporadic (19–21) and familial (22) SRS cases but no mutation was demonstrated. Fedoriw *et al*. (23) showed that CTCF protects the mouse ICR1 from *de novo* methylation during oocyte growth and is required for normal pre-implantation development. Indeed, reduced CTCF levels in oocytes result in gain of methylation of the CTCF binding sites (23). The putative role of CTCF in human disorders has not been extensively investigated. However, deleterious mutations of *CTCF* have been demonstrated in several tumors, including Wilms' tumors (24).

In this study, we investigated the cause of abnormal ICR1 imprinting by analyzing both ICR1 and the *CTCF* gene in patients with ICR1 gain or loss of methylation. We identified ICR1 genetic abnormalities in four BWS patients, including a familial case, and one SRS patient. In this report, we also describe for the first time ICR1 genetic defects involving one of the OCT-binding sequences and a SOX sequence suggesting that these *cis* acting elements are required in establishing and/or maintaining the imprints at 11p15 ICR1.

RESULTS

In order to determine the mechanism(s) underlying the ICR1 DNA methylation defect in SRS and BWS patients, we screened the *CTCF* gene (BWS patients) and the ICR1 domain (BWS and SRS patients) for mutations and deletions.

Imprinting status at the 11p15 region in the BWS and SRS cohort

All BWS patients displayed gain of methylation of the ICR1 and *H19* promoter regions as determined by Southern-blotting with methylation indexes in blood cells varying between 63 and 94% [normal controls: 53.9 ± 2% (49–57%)]. Other tissues [normal kidney ($n = 1$), tongue ($n = 2$), Wilms' tumor ($n = 2$)] were available for four patients and the same DNA methylation defect was found in tissues other than blood. RNA was available for three patients (leukocytes: $n = 1$; tissues: $n = 2$). Expression of *IGF2* was biallelic in the two patients informative for the *Ava*II/*Apa*I polymorphism in exon 9 (one patient's Wilms tumor and BWS12's blood cells). *H19* expression was abrogated in two tissue samples (BWS5's tongue tissue and another patient's Wilms tumor.

All SRS patients displayed loss of methylation of the ICR1 and *H19* promoter regions with methylation indexes in blood cells varying between 8 and 34%.

The methylation status at ICR2 was in the normal range for both BWS and SRS patients (BWS: 52.5 ± 4%; SRS: 51.4 ± 3.4%; controls: 51.6 ± 2.5%).

Mutation analysis of CTCF

Since CTCF binding is required for the prevention of *de novo* methylation at ICR1 and some *CTCF* mutations have been described in Wilms' tumors (24) (a very common tumor in BWS patients with ICR1 gain of methylation) (4,5), we screened for mutations of the *CTCF* gene, that could affect the structure of the zinc fingers, in all BWS patients with ICR1 gain of methylation. We sequenced all coding exons (exons 3–12) and flanking intronic regions.

No change in the coding sequence of the *CTCF* gene was found in any of the BWS patients. Only a single-nucleotide variation with respect to the reference sequence (NM_006565.2) was found in the 3′-UTR (Exon 12, rs6499137, G/T) of three patients. These results indicate that *CTCF* gene mutations are not a common cause of ICR1 gain of methylation in BWS.

ICR1 deletions and mutations in BWS and SRS patients

Familial BWS case. Two patients (BWS15 and BWS16) were siblings and the family pedigree is shown in Figure 1A. Patient II-1 (BWS15) was born after 39 weeks of gestation from non-consanguineous parents. The clinical presentation at birth included macrosomia (birth weight 5500 g, +5 SD), severe macroglossia, diastasis recti, nephromegaly, neonatal hypoglycemia and bilateral cryptorchidism (Table 1). A brother (II-3) displaying macrosomia (birth weight 5000 g, +3 SD), macroglossia and nephromegaly, died early after birth. Another brother (II-5; BWS16) displayed the same phenotype as patient II-1 including macrosomia (+5.2 SD) and nephromegaly (Table 1). Both patients (II-1 and II-5) underwent partial glossectomy within the first months of life. None of

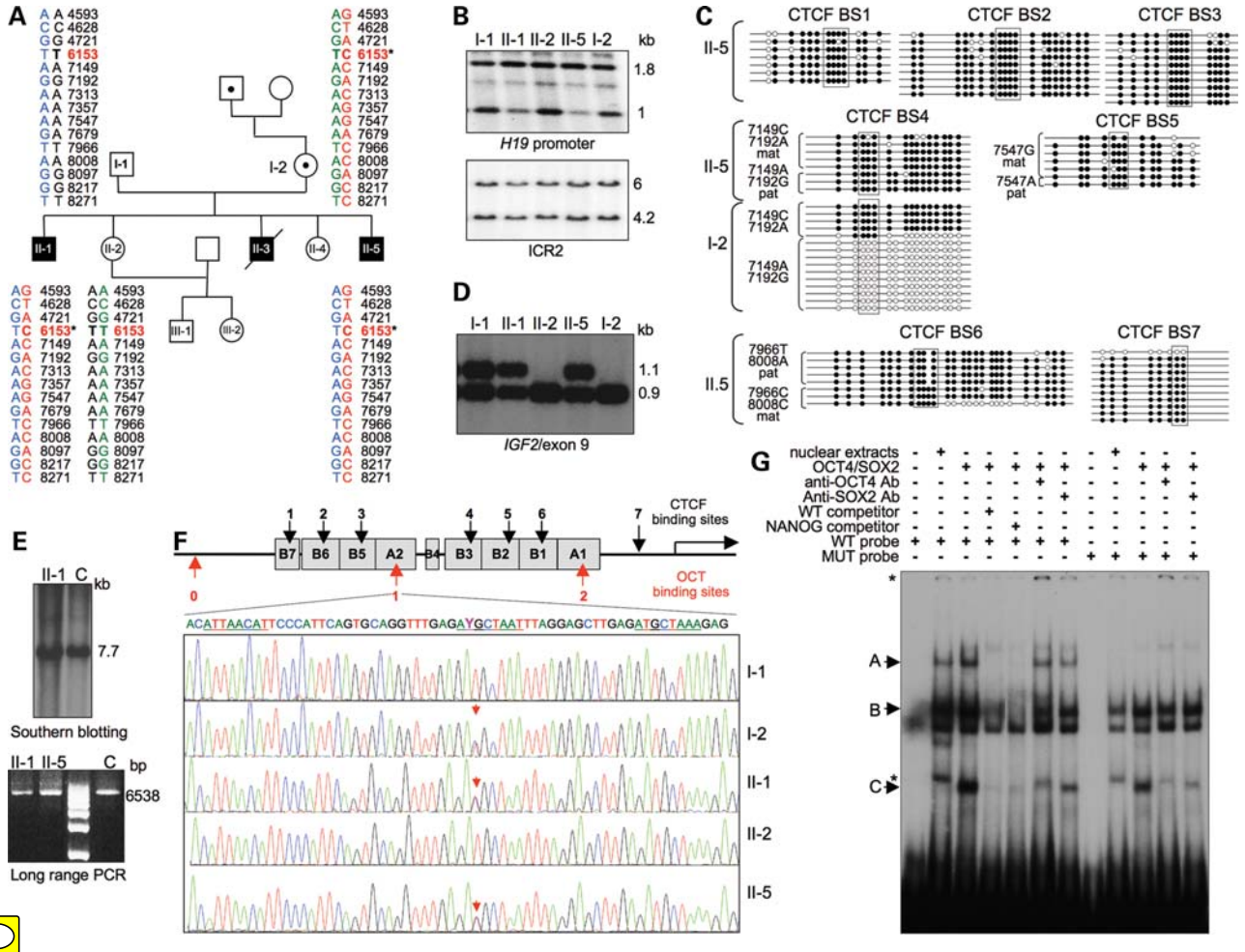

Figure 1. Familial BWS case. (**A**) Pedigree of the familial BWS case and segregation of ICR1 haplotypes as determined by SNP test. The SNPs and their positions in the AF125183 sequence are indicated. Carriers of the mutation are indicated. (**B**) Methylation at the *H19* promoter and ICR2, assayed by methyl-sensitive Southern blotting using genomic DNA from the indicated individuals. The upper bands (1.8 and 6 kb) are methylated and correspond to the paternal (*H19* promoter) and maternal (ICR2) alleles, respectively. The lower bands (1 and 4.2 kb) are unmethylated and correspond to the maternal (*H19* promoter) and paternal (ICR2) alleles, respectively. (**C**) DNA methylation profiles of the seven CTCF binding sites and flanking regions determined by bisulfite sequencing in patient II-5 and his mother (CTCF binding site 4). Each line corresponds to an individual cloned DNA fragment and each circle represents a CpG dinucleotide. Methylated CpGs are indicated by filled circles and unmethylated CpGs by open circles. Maternal and paternal alleles were distinguished by known single nucleotide polymorphisms. The CpG included in the CTCF binding sites are framed. (**D**) Genotyping at the polymorphic *Ava*II/*Apa*I site in exon 9 of the *IGF2* gene did not show allelic imbalance, ruling out a paternal duplication or a paternal trisomy. (**E**) Southern-blotting and long-range PCR (positions 2704–9241 of the AF125183 sequence) ruling out a microdeletion. (**F**) Identification and localization of the heterozygous mutation (6153 (T > C), numbered according to AF125183). The ICR1 domain is arranged in two repeat blocks containing A- and B-repeat elements. Six target sites for CTCF, numbered above the repeat blocks, are present within B-repeat elements and a seventh target site is positioned between the repeat blocks and the *H19* transcription start site. ICR1 contains three evolutionary conserved octamer motif OCT-binding sites (numbered below the repeat blocks). The second OCT-binding site contains three octamer motifs (underlined). The mutation is located within the second octamer of the second OCT-binding site (A2 repeat). (**G**) Band shift assays of the wild-type (WT) probe and the probe mutated at position 6153 (T > C) of the A2 OCT-binding site (MUT). Arrows mark protein-DNA complexes (A, B and C). Asterisks show supershifted complexes. Competitor: cold wild-type or NANOG competitor added at ×50 molar excess.

them (29 and 17 years old, respectively) developed a Wilms' tumor. There was no familial history evocative of BWS on the mother's side. The father I-1 was born with severe macrosomia (+5.4 SD) but did not display any other BWS phenotypes except a supernumerary nipple. The two sisters (II-2 and II-4) as well as the mother (I-2) were born with a normal birth weight and were phenotypically normal. Sequencing of the *Glypican 3* gene in probands ruled out a Simpson–Golabi–Behmel syndrome. Analysis of the 11p15 region showed a gain of methylation at all CTCF binding sites and the *H19* promoter with a normal methylation pattern at ICR2 (Fig. 1B and C). The 11p15 methylation status was normal in both parents and one of the sisters, whom DNA was available (Fig. 1B). Metaphase FISH for *IGF2* excluded trisomy (data not shown) and genotyping at a polymorphic *Ava*II/*Apa*I *IGF2* exon 9 site excluded a *cis*-duplication of the ICR1 region (Fig. 1D). Analysis of ICR1 by Southern blotting and long-range PCR was normal (Fig. 1E), eliminating a microdeletion or a cryptic chromosomal alteration at ICR1. Sequencing of ICR1 showed that the two affected brothers (patients II-1 and II-5) carried a maternally inherited single nucleotide variation (T>C) within the second octamer motif of the OCT-binding sequence 1 located in repeat A2 (position 6153 of the reference sequence AF125183) (Fig. 1F). The father and

Table 1. Clinical features of patients with Beckwith–Wiedemann and Silver–Russell syndromes

Phenotype	BWS All BWS patients	BWS5	BWS12	BWS13	BWS15[a]	BWS16[a]	SRS Phenotype	All SRS patients	SRS13
n	21						n	16	
Sex F/M	11/10	F	F	M	M	M	sex F/M	7/9	F
Macrosomia, *n* (%)	19/21 (90.5)	+2.7 SD	+4.4 SD	+4.3 SD	+5 SD	+5.2 SD	IUGR, *n* (%)	16/16 (100)	−2 SD
Macroglossia, *n* (%)	18/21 (86)	+	+	+	+	+	Post-natal growth retardation, *n* (%)	16/16 (100)	+
Abdominal wall defect, *n* (%)	13/21 (62)	+	+	+	+	+	Relative macrocephaly at birth, *n* (%)	16/16 (100)	+
Diastasis recti, *n* (%)	9	+	+	+	+		Facial dysmorphy, *n* (%)	16/16 (100)	+
Umbilical hernia, *n* (%)	4	+					Body asymmetry, *n* (%)	13/16 (81)	−
Exomphalos, *n* (%)	0						Feeding difficulties, *n* (%)	12/14 (86)	+
Organomegaly, *n* (%)	16/18 (89)	+	+	+	+	+	Developmental delay, *n* (%)	3/14 (21)	−
Body asymmetry, *n* (%)	7/21 (33)	+	−	−	−	−	Clinodactyly, *n* (%)	10/13 (77)	+
Hypoglycemia, *n* (%)	5/19 (26)	−	−	−	+	+			
Ear abnormalities, *n* (%)	7/18 (39)	−	+	−	−	−			
Wilms' tumor, *n* (%)	7/20 (35)	−	+	−	−	−			

IUGR, intrauterine growth retardation.
[a]Siblings.

the unaffected sister were homozygous for the T allele, corresponding to the normal sequence. This variation was not found neither in a control population ($n = 92$ chromosomes) nor in all public databases and is therefore likely to be deleterious. As grandparents' samples were not available, the determination of the grandparental origin of the mutated chromosome was assessed by combined DNA methylation analysis and SNP allele discrimination in the mother. Assuming that the grand paternal allele was methylated in the unaffected mother, we analyzed by bisulfite sequencing the fourth CTCF binding site in the mother and showed that the 7149C/7192A sequences were methylated (Fig. 1C). Therefore, the mutation in the probands originated from the maternal grandfather. Whether this single mutation disrupts binding of nuclear protein factors was determined by EMSA. The ^{32}P-labeled wild-type probe formed three complexes (A, B and C) with mouse ES cell nuclear extracts or the cell lysate overexpressing human OCT4 and SOX2 proteins (OCT4/SOX2) (Fig. 1G). The interactions (complexes A, B and C) were competed away by an excess of cold wild-type probe or control (NANOG) probe. Excess of mutated probe competed complexes B and C but did not affect complex A (data not shown). The complexes were partially neutralized (complex B) or supershifted (complex C) in the presence of an anti-OCT4 polyclonal antibody (Fig. 1G). One of the protein-DNA complexes (upper band, complex A) was not observed when a ^{32}P-labeled mutated probe (6153 T > C) was used (Fig. 1G) with both mouse ES cell nuclear extracts and human OCT4/SOX2 proteins, demonstrating that the mutation disrupts the binding of nuclear factors, most likely OCT4.

Sporadic BWS cases. Three BWS patients with apparently sporadic BWS displayed ICR1 genetic abnormalities.

Patient BWS12. The female patient has been previously reported (patient P2) (25,26). She was born at term with macrosomia [birth weight 5500 g (+4.4 SD), birth length 56 cm (+2.6 SD)]. She also displayed macroglossia, diastasis recti, organomegaly (kidneys and spleen) and ear pits. No hemihyperplasia was observed (Table 1). There was no familial history evocative of BWS although on the mother's side, a few relatives were born with macrosomia (Fig. 2A). The patient was diagnosed with a Wilms' tumor when she was 2 years old and underwent a right nephrectomy followed by chemotherapy. She also underwent partial glossectomy when she was 6 years old. Her growth velocity was regular (+2.5 SD) and her final height was 179 cm (+2.8 SD), far above her target height (−0.4 SD).

Direct DNA sequencing of the ICR1 domain identified a 212 bp deletion within the A2 domain (breakpoint residues 5930/6141 according to the reference sequence AF125183) deleting the first octamer motif of the second OCT-binding sequence and conserving the second and the third octamer motifs (Fig. 2B). The mother did not display the deletion (Fig. 2C) and PCR analysis showed normal allelic inheritance of microsatellite loci (data not shown). Bisulfite sequencing was performed at CTCF binding sites 4 and 6 and demonstrated a complete gain of methylation on the maternal allele (Fig. 2D).

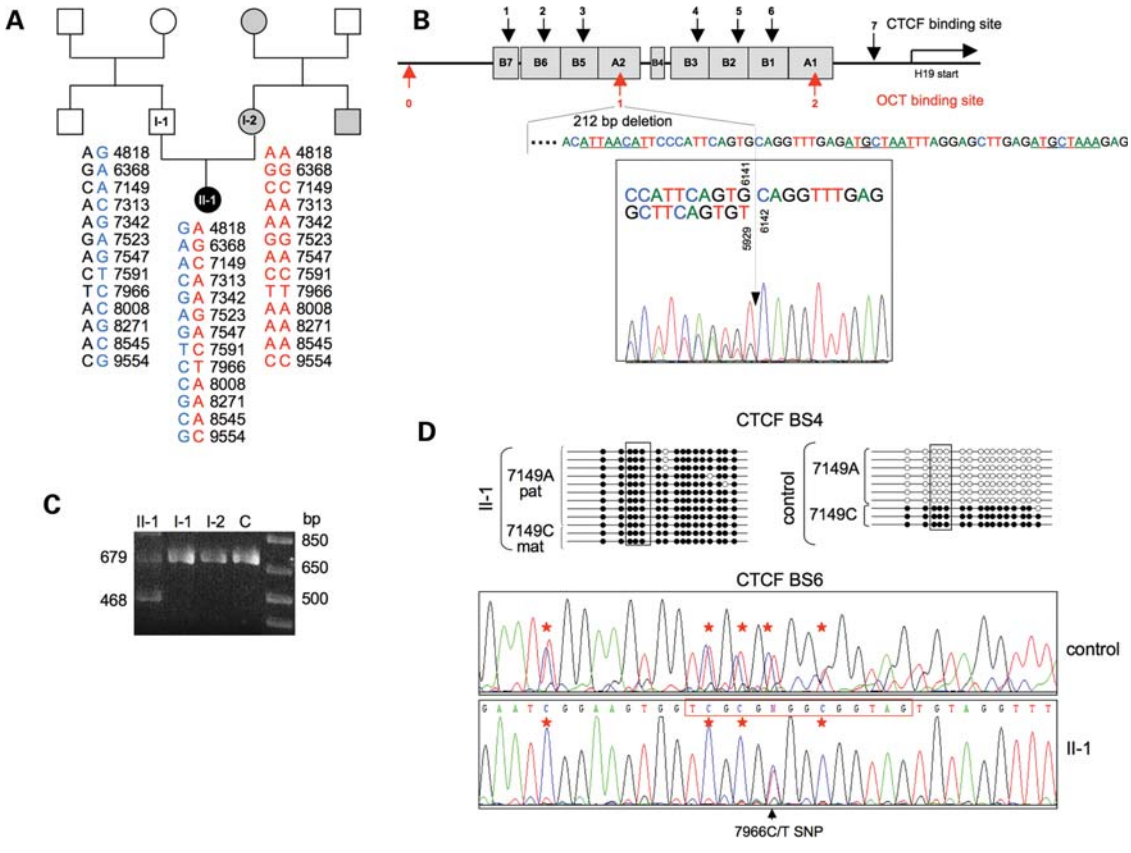

Figure 2. ICR1 microdeletion in BWS12. (**A**) Pedigree of the family and segregation of ICR1 haplotypes as determined by SNP test. Individuals in grey displayed macrosomia at birth. (**B**) Identification and localization of the microdeletion. The 212 bp microdeletion is located within the A2 domain (breakpoints at 5930 and 6141, numbered according to AF125183). As shown on the chromatogram, the microdeletion deletes the first octamer motif of the second OCT-binding sequence and conserves the second and the third octamer motifs. (**C**) Gel image of the PCR products (positions 5781–6459 of the AF125183 sequence) identifying the deletion and showing that the mother does not display the deletion. (**D**) DNA methylation profiles at CTCF binding sites 4 and 6 and flanking regions determined by bisulfite sequencing in patient II-1 and a control subject. For CTCF binding site 6, direct DNA sequencing was performed on bisulfite treated DNA. In the control subject, DNA sequencing shows a thymidine and a cytosine peaks at CpG sites (stars) corresponding to methylated and unmethyated alleles. In patient II-1, DNA sequencing shows only cytosine peaks (stars) at CpG sites, demonstrating a complete gain of methylation; the 7966 SNP shows that both alleles are equally represented.

Patient BWS13. The male patient II-3 (Fig. 3A) was born after 38 weeks of gestation from a non-consanguinous union. The pregnancy was complicated at the 22nd week of gestation by macrosomia, enlarged echogenic kidneys and nephrotic syndrome. Patient II-3 is the third of five siblings. None of the other siblings display any clinical features of BWS and all had normal birth weight. A sixth 46 XY pregnancy was terminated at a term of 25 weeks because of renal agenesis and lung hypoplasia. BWS diagnosis was placed in patient II-3 on the basis of the presence of macrosomia [birth weight 4860 g (+4.3 SD), birth length 55 cm (+2.8 SD)], macroglossia, diastasis recti and nephromegaly (Table 1). Mild dysmorphism such as slight ephicantus and malar hypoplasia were present. No haemangioma or hemihyperplasia were observed. Since birth, the patient has undergone follow-up with periodical ultrasound monitoring and did not develop a Wilms' tumor. At last examination ($5^{3/12}$ years), macroglossia was still present and the patient had developed obesity [114 cm (+1.1 SD), 24.7 kg (+5 SD), BMI 19].

Long-range PCR identified a 1.8 kb deletion (Fig. 3C). Sequencing of the deleted fragment, following gel purification and cloning, showed that the 1.8 kb deletion fused repeats B6 and B3 (breakpoint range residues 5068–5086/6901–6919 according to the reference sequence AF125183) deleting CTCF binding sites 2 and 3 (Fig. 3B). The deletion was maternally inherited (Fig. 3C). Analysis by quantitative PCR confirmed the deletion (Fig. 3D). Southern blotting following digestion with *Pst*I and *Sma*I and hybridization with a probe recognizing two ICR1 loci (B6-A2 and B2-A1) (Fig. 3B and E) allowed to validate the inheritance of the deletion and showed that the deletion was associated with the maternal abnormal methylated allele. The patient and his mother displayed one additional band (2778 bp) corresponding to the deleted allele (which misses the *Sma*I site located in B6) (Fig. 3B and E). The presence of the two 2463 and 2149 bp bands (corresponding to two *Pst*I methylated fragments on the non-deleted allele) in the patient and the absence of them in his mother demonstrate that the mother inherited the abnormal allele from her father. Investigation of the four siblings and the fetus showed that none of them display the deletion.

Direct sequencing of the ICR1 domain in patient II-3 also showed a maternally inherited single variation within the B1 domain (position 7916) (Fig. 3A) that is not a known SNP and was not found in a control population (Table 2).

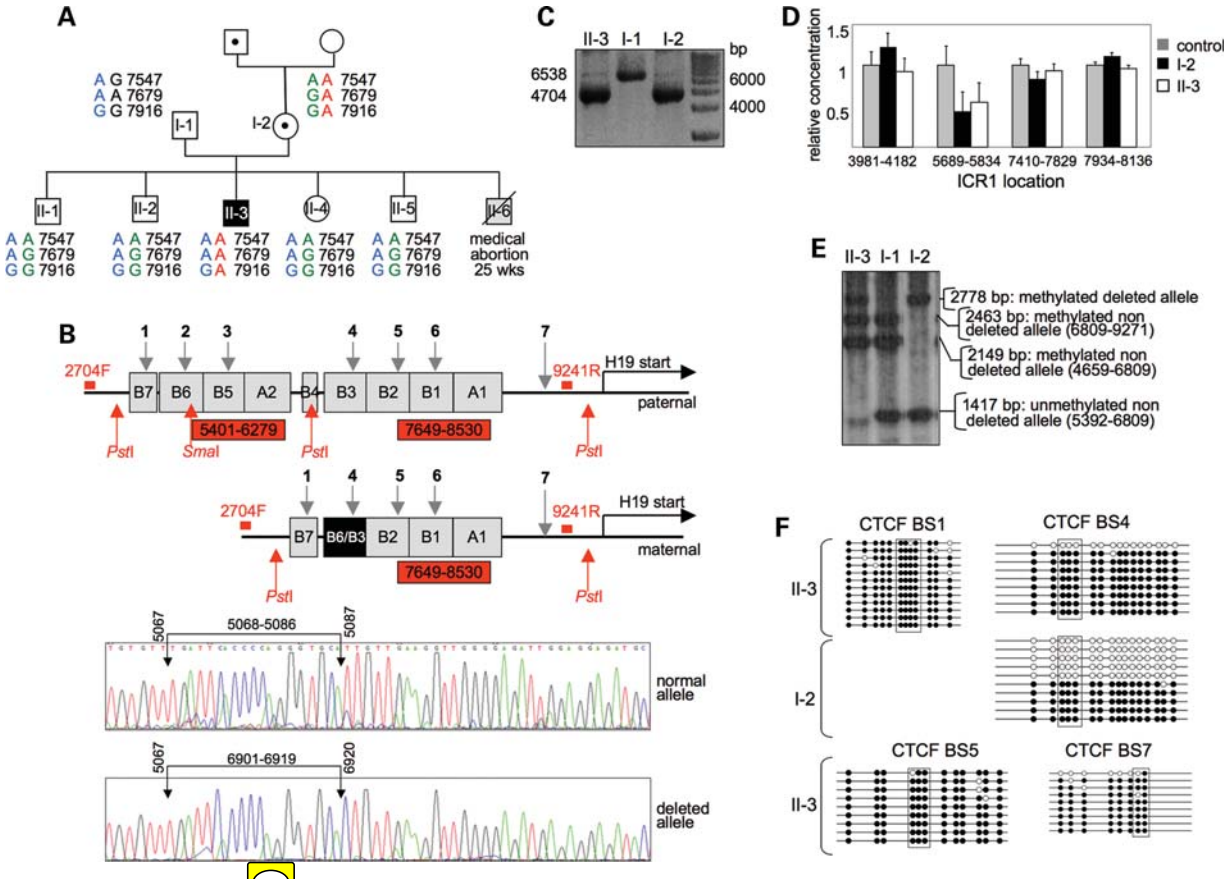

Figure 3. ICR1 deletion in BWS13. Pedigree of the family and segregation of ICR1 haplotypes as determined by SNP test. Carriers of the deletion are indicated. Medical abortion was performed on individual II-6 because of renal agenesia. (**B**) Characterization of the deleted allele. Location of the primers used for long-range PCR and the probe used for hybridization are indicated. Position of the breakpoints (at 5068/5086 and 6901/6919, numbered according to AF125183) have been identified after cloning and sequencing both alleles and are highlighted on the chromatograms. The microdeletion deletes two CTCF target sites (2 and 3). (**C**) Gel image of long-range PCR products (positions 2704–9241 of the AF125183 sequence) showing an abnormal 4.7 kb allele in addition to the wild-type 6.5 kb allele and the transmission of the deletion from the mother. (**D**) Genomic real-time PCR quantification assay at different loci along the ICR1 domain confirmed the deletion and ruled out a trisomy or a duplication of the deleted domain. (**E**) Southern-blot following digestion with *Pst*I and *Sma*I in patient II-3 and his parents. The probe used for hybridization is shown on Figure 3B. (**F**) DNA methylation profiles of CTCF binding sites 1, 4, 5 and 7 and flanking regions determined by bisulfite sequencing in blood cells from the propositus and his mother (CTCF binding site 4).

DNA methylation analysis was performed at CTCF binding sites 1, 4, 5 and 7 for patient II-3 and CTCF binding site 4 for his mother. Bisulfite sequencing demonstrated a gain of methylation at the various CTCF binding sites in patient II-3 (Fig. 3F).

Patient BWS5. The female patient II-2 (Fig. 4A) was born after 39 weeks of gestation. BWS diagnosis was placed on the basis of the presence of macrosomia [birth weight 4500 g (+2.7 SD) and birth length 54 cm (+1.8 SD)], macroglossia, left hemihypertrophy, umbilical hernia with diastasis recti and left inguinal hernia (Table 1). No haemangioma or ear anomalies were observed. Post-natal ultrasonography revealed hepatomegaly and calicopyelic dilatation of the left kidney. Partial glossectomy was performed at the age of 6 months. The patient was followed-up until the age of 19 years and did not develop a Wilms' tumor. Direct DNA sequencing of the ICR1 domain identified a 8 bp deletion (residues 7277–7284 according to the reference sequence AF125183) within the B3 repeat (Fig. 4B), corresponding to a putative consensus site (CATTCATG) for the SOX2 transcription factor. The microdeletion was maternally inherited (Fig. 4B). Bisulfite sequencing was performed at all CTCF binding sites and demonstrated a similar gain of methylation on the maternal allele at all CTCF binding sites (Fig. 4C). Bisulfite sequencing of the fourth CTCF binding site in the mother confirmed that the deleted allele (7149C/A7192A) was the methylated allele (Fig. 4C). Therefore, the deletion in patient BWS5 was derived from the maternal grandfather.

SRS cases

One SRS patient displayed a single nucleotide variation.

Patient SRS13. The female patient II-2 (Fig. 5A) was born after a spontaneous monozygotic twin pregnancy. The twin sister died *in utero* between 12 and 20 weeks. Because of intrauterine growth retardation, a cesarean section was performed at 31 weeks of pregnancy. The proband had a birth weight of 1140 g (−2 SD), birth length of 38 cm (−1.9 SD) and a skull circumference of 28 cm (−0.5 SD). Pathologic examination showed a monochorionic, diamniotic placenta.

Table 2. Sequence variations of the ICR1 region in BWS and SRS patients

Patient	Phenotype	Variation	Position (Acc AF125183)	Domain	Transmission	% heterozygosity (x/n chromosomes)
BWS5	BWS	del 8 bp[a]	7277–7284	B3/SOX motif	Maternal	0 (0/92)
BWS13	BWS	del 1.8 kb[a]	5068–5086/6901–6919	B6>B3	Maternal	0 (0/96)
BWS13	BWS	G > A[a]	7916	B1/5′ of CTCFBS6	Maternal	0 (0/96)
BWS12	BWS	del 212 bp[a]	5930–6141	A2/OCT motif	*de novo*	0 (0/92)
BWS15, BWS16	Familial BWS	T>C[a]	6153	A2/OCT motif	Maternal	0 (0/92)
SRS13	SRS	G > T[a]	9048	3′ of CTCFBS7	*de novo*	0 (0/96)
SRS14	SRS	C > T[b]; ss 161109780	5269	B6/5′ of CTCFBS2	Maternal	4.2 (2/96)
BWS21	BWS	C > A[b]; ss 161109781	7648	B2/3′ of CTCFBS5	NA	6.5 (3/92)

CTCFBS, CTCF binding site; NA, not available.
[a]Not found in the control population.
[b]New polymorphisms.

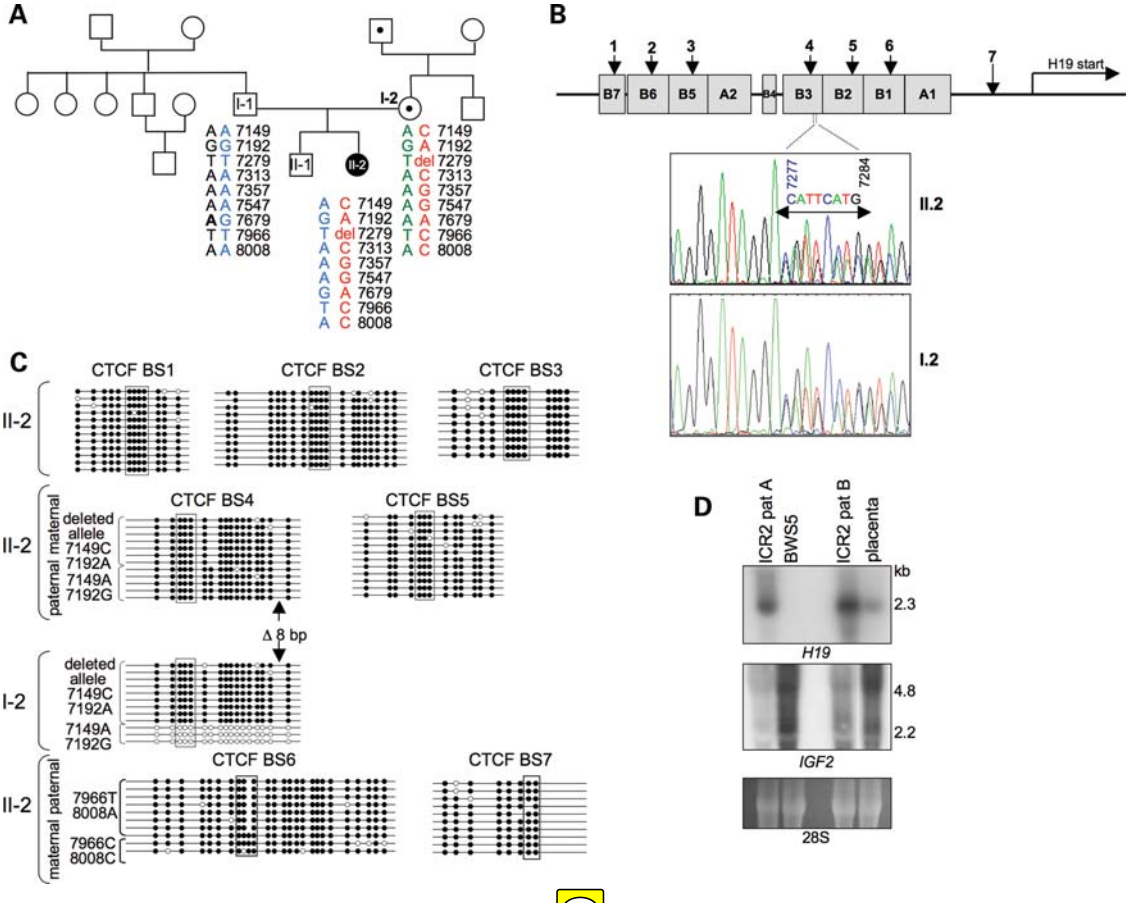

Figure 4. ICR1 microdeletion in BWS5. (**A**) Pedigree of the family and segregation of ICR1 haplotypes as determined by SNP test. Carriers of the deletion are indicated. (**B**) Identification and localization of the microdeletion in patient BWS5 and her mother. The microdeletion is located within the B3 domain; as shown on chromatogram, the breakpoints are indicated by arrows at 7277 and 7284, numbered according to AF125183. (**C**) DNA methylation profiles of the seven CTCF binding sites and flanking regions determined by bisulfite sequencing in tongue tissue from patient BWS5 and blood from her mother. Maternal and paternal alleles were distinguished by known single-nucleotide polymorphisms. (**D**) Northern blot analysis of IGF2 and H19 gene expression in tongue tissue from patient BWS5, tongue tissues from two BWS patients with ICR2 loss of methylation and normal methylation at ICR1 and a normal placenta sample.

In the first 8 years, patient SRS13 displayed post-natal growth retardation (weight −2.9 SD, height −3.6 SD, BMI −1.8 SD, head circumference −1.2 SD) and mild feeding difficulties (Table 1). Metabolic and endocrine investigations showed no abnormalities. SRS was diagnosed at 8 years of age on the basis of post-natal growth retardation with conserved head circumference, bossed forehead, clinodactyly of the fifth digits, café au lait spots and slight school difficulties and was confirmed by analysis of the 11p15 region.

ICR1 analysis identified a single nucleotide variation [9048 (G > T)] (Fig. 5B) that was not found in a control population ($n = 96$ chromosomes) or in public databases and is therefore

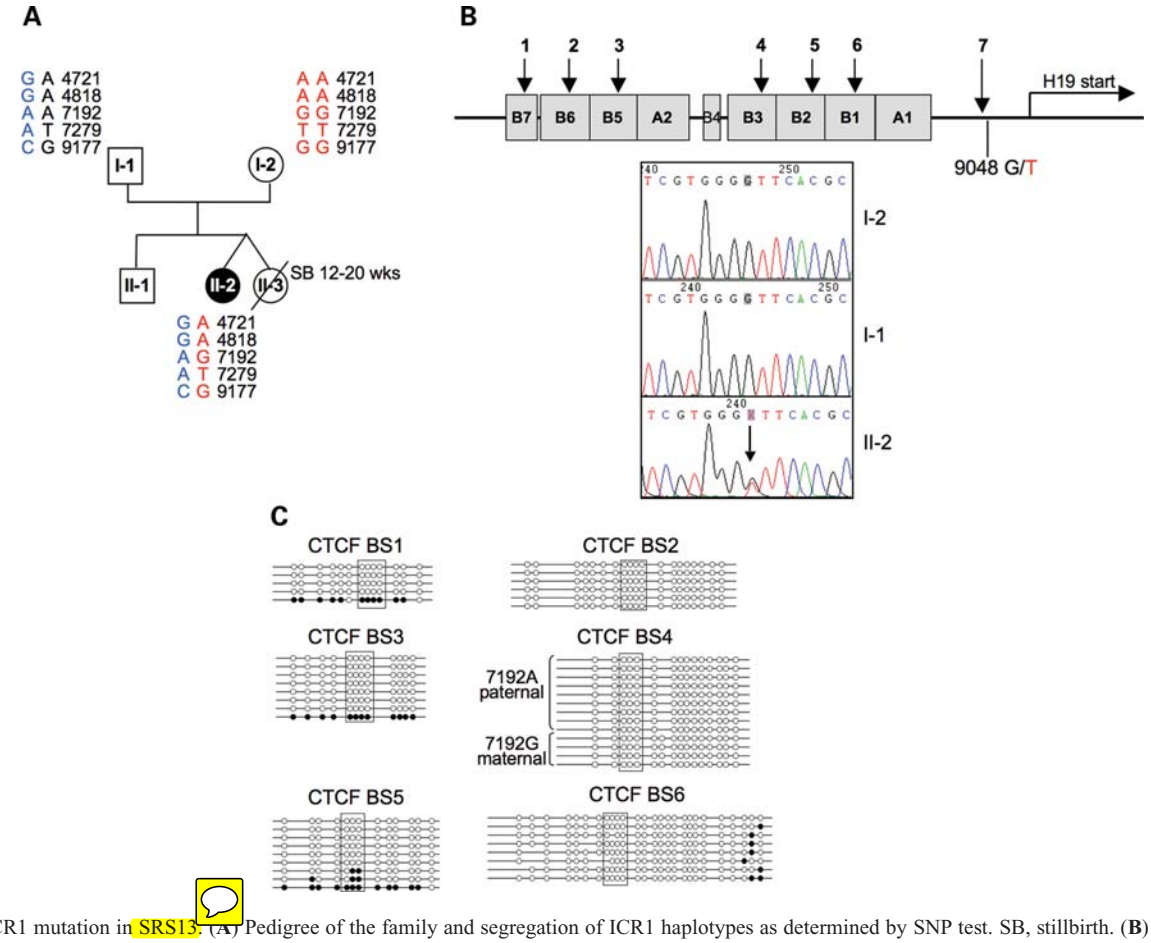

Figure 5. ICR1 mutation in SRS13. (**A**) Pedigree of the family and segregation of ICR1 haplotypes as determined by SNP test. SB, stillbirth. (**B**) Identification and localization of the heterozygous mutation (9048 (G > T), numbered according to AF125183). (**C**) DNA methylation profiles of the CTCF binding sites 1–6 and flanking regions determined by bisulfite sequencing in blood cells. Maternal and paternal alleles were distinguished by known single-nucleotide polymorphisms.

unlikely to be a polymorphism. Parental analysis showed that neither the father nor the mother displayed the mutation (Fig. 5B) and multiplex PCR analysis of microsatellite loci confirmed the paternity (data not shown), suggesting that the patient displays a *de novo* mutation. Bisulfite sequencing demonstrated a loss of methylation at CTCF binding sites and the presence of a SNP at 7192 (CTCF binding site 4) confirmed a loss of methylation on the paternal chromosome (Fig. 5C).

Two other patients (1 SRS and 1 BWS) displayed new single nucleotide variations [positions 5269 in B6 (ss161109780) and 7648 in B2 (ss161109781)] (Table 2) that correspond to rare polymorphisms as they were also detected in control samples (informativity rate of 4.2 and 6.5%, respectively).

All single nucleotide variations and deletions and their parental inheritance when available are summarized in Table 2.

DISCUSSION

Abnormal methylation of the 11p15 ICR1 *H19/IGF2* imprinted domain accounts for ∼10% of BWS patients and 60% of SRS patients. Little information is available regarding the mechanism of ICR1 DNA methylation defects. Several deletions (1.4 to 2.2 kb) removing part of ICR1 have been described in a few BWS familial cases with dominant maternal transmission (15–18). Very recently, Scott *et al.* (27) showed that constitutive ICR1 imprinting abnormalities (including a 5.3 kb deletion and a 2.9 kb insertion) also occur in apparently sporadic Wilms' tumors. Even less is known regarding the mechanism of ICR1 loss of methylation in SRS patients. Engel *et al.* (14) previously showed that mutations of CpG dinucleotides in the mouse *H19* DMD result in a growth retardation phenotype when paternally inherited. However, attempts to identify ICR1 mutations in SRS patients, including a few familial cases, were negative (19–22).

In this study, we investigated ICR1 and the *CTCF* gene in patients with ICR1 DNA methylation defects. Missense mutations of the *CTCF* gene have been previously described in several tumors including two Wilms' tumors (24). The CTCF protein can use different combinations of the zinc-finger domains to bind different DNA target sequences and it was recently shown that the seventh zinc finger (encoded by exons 5 and 6) is specifically involved in CTCF binding at the *Igf2/H19* ICR1 locus (28). Therefore, we hypothesized that deleterious mutation of *CTCF* might confer a selective

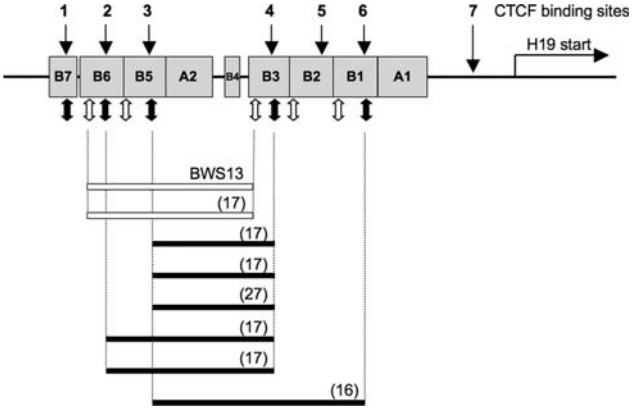

Figure 6. Representation of the hot spot deletion breakpoints within the ICR1 domain. Organization of the wild-type ICR1 domain and localization of two highly repetitive sequences: AAGTGGCCGCGCGGCGGCAGTGCAGGCTC (black arrows) and GATTCACCCCAGGGTGCA (white arrows). Localization of BWS13's ICR1 deletion and deletions previously described (references).

growth advantage and account for some BWS with ICR1 gain of methylation. No mutation was found in BWS patients and our data are consistent with a recent publication (18). Regarding ICR1 in SRS patients, only one *de novo* mutation was found in a non-familial SRS case. This new mutation did not involve a CTCF binding site. The relevance of the mutation would ultimately be validated by chromosome conformation capture assays and directed mutagenesis.

Interestingly, we show in this study that mutations and deletions within ICR1 are relatively common in BWS patients and account for 20% of BWS patients with ICR1 gain of methylation. One patient displayed a 1.8 kb deletion fusing B6 and B3 repeats, similar to an unrelated familial case described by Sparago *et al*. (17). Constitutive ICR1 deletions previously described in BWS patients were deletions removing 1.4–2.2 kb at the core of ICR1, fusing two repeat blocks and abolishing one to three CTCF target sites (15–17). More recently, a larger deletion of 5.3 kb removing both repeat blocks and a 2.9 kb insertion (corresponding to the duplication of two fused repeats) were described in patients with non-syndromic Wilms' tumors (27). The ICR1 sequence is highly polymorphic and repetitive. Analysis of the breakpoint locations in patient BWS13 and in the various deletions previously described showed that most of them occurred at two highly repetitive sequences dispersed within the B-repeats (Fig. 6). The repetition of these DNA sequences might expose to a higher rate of recombination and therefore account for the incidence and location of ICR1 deletions. Lercher *et al*. (29) previously suggested that most imprinted chromosomal regions exhibit higher recombination rates. More recently, Sandovici *et al*. (30) confirmed an excess of hot-spots of recombination at imprinted loci, particularly at the 11p15 region, compared with the rest of the genome. Very interestingly, new genetic defects involving OCT or SOX motifs were found in three of four BWS patients. In the familial case, three brothers displayed an overgrowth phenotype when two sisters were unaffected. The family was initially investigated for the X linked Simpson–Golabi–Behmel syndrome but the sequencing of the *Glypican 3* gene was normal. Instead, analysis of the 11p15 region showed that the affected brothers displayed a gain of methylation at ICR1. No genetic defect involving the *CTCF* gene or the CTCF binding sites was shown in this family. In addition to the B repeats containing CTCF binding sites, the ICR1 domain also displays two A repeats which include putative OCT-binding domains with conserved octamer motifs (31). Sequencing of the A repeats in the BWS familial case identified a maternally transmitted mutation at a very well conserved residue within the second octamer motif of the OCT-binding sequence located in repeat A2. By gel shift assay, we showed that this mutation impairs the binding of human OCT4/SOX2 proteins suggesting that these transcription factors are involved in imprinting control of the ICR1 domain. A second genetic defect involving the OCT-binding sequence of the A2 domain was identified in a sporadic BWS case. The 212 bp deletion identified in this second patient removes the first octamer motif of the OCT-binding sequence located in repeat A2. In this case, the deletion occurred *de novo*. No mutation or deletion was found within the two other OCT-binding sequences located upstream of the repeat blocks and within A1. Moreover, we identified a very small deletion of 8 bp (CATTCATG) within the B3 domain corresponding to a putative consensus site for SOX2.

In the mouse, the well-conserved octamer motifs have been shown to bind OCT-family proteins and to maintain the unmethylated status of the neighbouring B-repeats of the maternal allele (31). Indeed, mutations of the dyad OCT-binding domains in mouse cells prevent the maintenance of the unmethylated status of the maternal allele, despite normal binding of the CTCF protein to CTCF binding sites (31). This strongly suggests that the OCT-binding domains are essential *cis*-acting sequences for ICR1 to function as an insulator. The critical role of OCT and SOX binding sequences was recently emphasized at the human Angelman syndrome imprinting center (32). The authors identified two OCT and one SOX sequences on the human Angelman syndrome imprinting centre (AS-IC). By mutating separately those three sequences, they showed that the mutation of either OCT or SOX sites resulted in a significant AS-IC maternal gain of methylation in oocytes (32), suggesting that a protein complex of OCT and SOX plays a role in determining the methylation status of AS-IC. It is also noteworthy that some Angelman patients display a 4 bp deletion within this SOX motif (33). Further studies will determine how structural abnormalities at OCT or SOX binding sites can affect the DNA methylation status at ICR1 and whether it occurs through a loss of interaction with the CTCF protein. Binding sites for Oct4 and Sox2 were recently identified within the X chromosome inactivation center and both Oct4 and Sox2 were shown to be involved in the regulation of X-chromosome inactivation (34). Moreover, Oct4 complexes with CTCF through direct protein–protein interactions and depletion of Oct4 results in the inactivation of both X chromosomes (34). It will therefore be important to investigate if OCT4 and/or SOX2 interact with CTCF at ICR1 and how a putative loss of interaction can affect the chromatin organization of the ICR1 domain.

In conclusion, we described new mutations and deletions within ICR1 in four BWS and one SRS patients which, for most of them, involve other domains that CTCF binding sites. BWS patients with ICR1 gain of methylation have a high risk of Wilms' tumor and an accurate molecular diagnosis is particularly important for genetic counseling and tumor surveillance. Those new data clearly complicate the investigation of such patients. Indeed, the search for mutation or deletion should not be conducted only in patients with a familial history of BWS, as some BWS patients with deletions had no familial history (this study and 17). Moreover, routinely used diagnostic tools (such as methylation-specific multiplex ligation-dependent probe amplication) (35) would fail to identify some of these novel genetic defects. Further, our data strongly suggest that other *cis*-acting elements (OCT- and SOX-binding sequences) than CTCF binding sites might participate in the regulation of imprinting at ICR1. Future studies will specifically address the timing and the precise mechanism(s) involving the OCT/SOX transcription factors in the regulation of ICR1 imprinting.

PATIENTS AND METHODS

Patients

This study was conducted in compliance with institutional guidelines for research studies in human genetics (approval no. 253/07, Alfred Hospital Ethics Committee and agreement numbers 681 and 682, Assistance Publique-Hôpitaux de Paris) and informed consent was obtained from participating individuals and/or their parents. The study population consisted of 37 patients with growth disorders caused by a DNA methylation defect of the 11p15 ICR1 domain.

Twenty-one patients were diagnosed with BWS. As reported previously (36), one of them was diagnosed during fetal life when an ultrasound scan revealed bilateral enlarged echogenic kidneys and macrosomia. After genetic counseling, the parents decided to have the pregnancy terminated. Two other patients were siblings and there were no other case evocative of BWS in the family. Seven of 20 (35%) BWS patients developed a Wilms' tumor (median age: 24 months; range: 14–39 months). One patient was treated at the age of 18 months by chemotherapy for bilateral nephroblastomasis. None of the remaining 12 patients developed a tumor (median follow-up: $10^{4/12}$ years; range 20 months–29 years).

Sixteen patients were SRS patients. All of them had a severe phenotype with severe growth retardation, relative macrocephaly at birth, facial dysmorphy and feeding difficulties; most of them (13/16) displayed body asymmetry. Two of them were discordant monozygotic twins and their respective twins were unaffected. Two SRS patients were born following the use of ovarian stimulation.

The phenotypes of BWS and SRS patients are summarized in Table 1.

DNA methylation analyses

Methyl-sensitive Southern blotting was used to analyze the methylation status of the 11p15 ICR1 telomeric domain and of the 11p15 ICR2 centromeric domain as previously described (4,7,8).

Bisulfite sequencing: 1 μg genomic lymphocyte DNA was bisulfite modified using the EZ DNA modification kit (Zymo Research, Orange, CA, USA) according to the manufacturer's instructions. CTCF binding sites 1–7 were amplified with primers previously reported (7,37,38) and additional primers listed in Supplementary Material, Table S1. The products were cloned into a pCR®II-TOPO vector (Invitrogen, Carlsbad, CA) according to the manufacturer's instructions. Ten to twelve clones were bidirectionally sequenced using the BigDye Terminator V3.1 cycle sequencing kit on the ABI 3100 automatic sequencer (Applied Biosystems, Foster City, CA, USA); sequences were analyzed with Chromas software (Applied Biosystems, Foster City, CA, USA) and the QUMA quantification software (quma.cdb.riken.jp) was used to represent the methylation status after bisulfite treatment.

Southern blot, PCR and DNA sequencing analyses of ICR1 and the *CTCF* gene

Enzymatic digestion and/or PCR were performed on genomic DNA extracted from leukocytes and/or tongue tissue as previously described (39). Analysis of ICR1 by *Apa*I digestion and Southern blotting was performed as previously described (7,15).

To investigate microdeletions within the 11p15 ICR1 region, long-range PCR amplifications were performed using the BIO-X-ACTTM Long DNA Polymerase (BIOLINE, Boston, MA, USA) and primers chosen along the ICR1 domain using Primer3 software (http://fokker.wi.mit.edu/primer3/input.htm; Supplementary Material, Table S1). To characterize finely the 1.8 kb deletion, both alleles (normal and deleted) were gel-purified using the Wizard® SV Gel and PCR Clean-Up System (Promega, Madison, WI, USA) and cloned into a pCR®II-TOPO vector (Invitrogen, Carlsbad, CA) according to the manufacturer's instructions. Cloned fragments were bi-directionally sequenced using the same protocol as above and results were analyzed with the Chromas software (Applied Biosystems, Foster City, CA, USA).

Standard PCR amplifications were performed to analyze the CTCF binding sites, the three OCT-binding sequences and the *CTCF* gene; primers used have been previously described (19,40,41) or are listed in Supplementary Material, Table S1.

RNA expression analysis of the *IGF2* and *H19* genes

Expression analysis of the *IGF2* and *H19* genes was carried out in tissues as previously described (39).

Electrophoretic mobility shift assays

293FT cells (Invitrogen) were transfected with pPS-human Oct4-T2A-RFP and pPS-human Sox2-T2A-RFP constructs (System Bioscience, CA, USA) by Lipofectamine 2000 (Invitrogen), according to the manufacturer's instructions. Forty-eight hours after transfection, cell lysates were prepared from the cells expressing human OCT4 and SOX2 proteins (OCT4/SOX2) (Supplementary Material, Fig. S1). The

EMSA oligonucleotides are listed in Supplementary Material, Table S1. Labeled double-strand probes (20–30 fmoles) were incubated at room temperature for 30 min with 5 μg of nuclear extracts from mouse ES cells or 5 μg of cell lysates expressing OCT4/SOX2 proteins in a buffer containing 12 mM HEPES, 60 mM KCl, 2 mM EDTA, 1 mM DTT, 3 μg of BSA and 1 μg poly[d(I-C)] in a volume of 20 μl. Supershifts and neutralizations were carried out with 1.5 μg of anti-OCT4 (Abcam, ab19857) or anti-SOX2 (R&D systems, AF2018, Minneapolis, MN, USA) antibodies. The reaction mixtures were separated on a 4% polyacrylamide gel, which was dried and exposed to a film.

WEB RESOURCES

The URLs for data presented herein are as follows: Online Mendelian Inheritance in Man (OMIM), http://www.ncbi.nlm.nih.gov/Omim; GenBank, http://ncbi.nlm.nih.gov/Genbank; accession codes: AF125183.

SUPPLEMENTARY MATERIAL

Supplementary Material is available at *HMG* online.

ACKNOWLEDGEMENTS

We thank the patients and their families and the physicians for patients' referrals and collection of clinical data. We also thank the DNA sequencing facility of the Baker IDI Heart and Diabetes Institute.

Conflict of Interest statement. None declared.

FUNDING

This work was supported by the National Health and Medical Research Council of Australia (Project grant 472637), the Baker IDI Heart and Diabetes Institute, the Institut National de la Santé et de la Recherche Médicale UMPC U938, Université Pierre et Marie Curie Paris 6 and Assistance Publique Hopitaux de Paris. M.E.S. received funding from the Libyan government.

REFERENCES

1. Reik, W. and Walter, J. (2001) Genomic imprinting: parental influence on the genome. *Nat. Rev. Genet.*, **2**, 21–32.
2. Delaval, K., Wagschal, A. and Feil, R. (2006) Epigenetic deregulation of imprinting in congenital diseases of aberrant growth. *Bioessays*, **28**, 453–459.
3. Gicquel, C. and Le Bouc, Y. (2006) Hormonal regulation of fetal growth. *Horm. Res.*, **65**, 28–33.
4. Gaston, V., Le Bouc, Y., Soupre, V., Burglen, L., Donadieu, J., Oro, H., Audry, G., Vazquez, M.P. and Gicquel, C. (2001) Analysis of the methylation status of the KCNQ1OT and H19 genes in leukocyte DNA for the diagnosis and prognosis of Beckwith-Wiedemann syndrome. *Eur. J. Hum. Genet.*, **9**, 409–418.
5. Cooper, W.N., Luharia, A., Evans, G.A., Raza, H., Haire, A.C., Grundy, R., Bowdin, S.C., Riccio, A., Sebastio, G., Bliek, J. *et al.* (2005) Molecular subtypes and phenotypic expression of Beckwith-Wiedemann syndrome. *Eur. J. Hum. Genet.*, **13**, 1025–1032.
6. Rossignol, S., Netchine, I., Le Bouc, Y. and Gicquel, C. (2008) Epigenetics in Silver-Russell syndrome. *Best. Pract. Res. Clin. Endocrinol. Metab.*, **22**, 403–414.
7. Gicquel, C., Rossignol, S., Cabrol, S., Houang, M., Steunou, V., Barbu, V., Danton, F., Thibaud, N., Le Merrer, M., Burglen, L. *et al.* (2005) Epimutation of the telomeric imprinting center region on chromosome 11p15 in Silver-Russell syndrome. *Nat. Genet.*, **37**, 1003–1007.
8. Netchine, I., Rossignol, S., Dufourg, M.N., Azzi, S., Rousseau, A., Perin, L., Houang, M., Steunou, V., Esteva, B., Thibaud, N. *et al.* (2007) 11p15 imprinting center region 1 loss of methylation is a common and specific cause of typical Russell-Silver syndrome: clinical scoring system and epigenetic-phenotypic correlations. *J. Clin. Endocrinol. Metab.*, **92**, 3148–3154.
9. Lucifero, D., Chaillet, J.R. and Trasler, J.M. (2004) Potential significance of genomic imprinting defects for reproduction and assisted reproductive technology. *Hum. Reprod. Update*, **10**, 3–18.
10. Murrell, A., Heeson, S. and Reik, W. (2004) Interaction between differentially methylated regions partitions the imprinted genes Igf2 and H19 into parent-specific chromatin loops. *Nat. Genet.*, **36**, 889–893.
11. Li, T., Hu, J.F., Qiu, X., Ling, J., Chen, H., Wang, S., Hou, A., Vu, T.H. and Hoffman, A.R. (2008) CTCF regulates allelic expression of Igf2 by orchestrating a promoter-polycomb repressive complex 2 intrachromosomal loop. *Mol. Cell. Biol.*, **28**, 6473–6482.
12. Qiu, X., Vu, T.H., Lu, Q., Ling, J.Q., Li, T., Hou, A., Wang, S.K., Chen, H.L., Hu, J.F. and Hoffman, A.R. (2008) A complex deoxyribonucleic acid looping configuration associated with the silencing of the maternal Igf2 allele. *Mol. Endocrinol.*, **22**, 1476–1488.
13. Pant, V., Mariano, P., Kanduri, C., Mattsson, A., Lobanenkov, V., Heuchel, R. and Ohlsson, R. (2003) The nucleotides responsible for the direct physical contact between the chromatin insulator protein CTCF and the H19 imprinting control region manifest parent of origin-specific long-distance insulation and methylation-free domains. *Genes Dev.*, **17**, 586–590.
14. Engel, N., West, A.G., Felsenfeld, G. and Bartolomei, M.S. (2004) Antagonism between DNA hypermethylation and enhancer-blocking activity at the H19 DMD is uncovered by CpG mutations. *Nat. Genet.*, **36**, 883–888.
15. Sparago, A., Cerrato, F., Vernucci, M., Ferrero, G.B., Silengo, M.C. and Riccio, A. (2004) Microdeletions in the human H19 DMR result in loss of IGF2 imprinting and Beckwith-Wiedemann syndrome. *Nat. Genet.*, **36**, 958–960.
16. Prawitt, D., Enklaar, T., Gartner-Rupprecht, B., Spangenberg, C., Oswald, M., Lausch, E., Schmidtke, P., Reutzel, D., Fees, S., Lucito, R. *et al.* (2005) Microdeletion of target sites for insulator protein CTCF in a chromosome 11p15 imprinting center in Beckwith-Wiedemann syndrome and Wilms' tumor. *Proc. Natl Acad. Sci. USA*, **102**, 4085–4090.
17. Sparago, A., Russo, S., Cerrato, F., Ferraiuolo, S., Castorina, P., Selicorni, A., Schwienbacher, C., Negrini, M., Ferrero, G.B., Silengo, M.C. *et al.* (2007) Mechanisms causing imprinting defects in familial Beckwith-Wiedemann syndrome with Wilms' tumour. *Hum. Mol. Genet.*, **16**, 254–264.
18. Cerrato, F., Sparago, A., Verde, G., De Crescenzo, A., Citro, V., Cubellis, M.V., Rinaldi, M.M., Boccuto, L., Neri, G., Magnani, C. *et al.* (2008) Different mechanisms cause imprinting defects at the IGF2/H19 locus in Beckwith-Wiedemann syndrome and Wilms' tumour. *Hum. Mol. Genet.*, **17**, 1427–1435.
19. Bliek, J., Terhal, P., van den Bogaard, M.J., Maas, S., Hamel, B., Salieb-Beugelaar, G., Simon, M., Letteboer, T., van der Smagt, J., Kroes, H. *et al.* (2006) Hypomethylation of the H19 gene causes not only Silver-Russell syndrome (SRS) but also isolated asymmetry or an SRS-like phenotype. *Am. J. Hum. Genet.*, **78**, 604–614.
20. Yamazawa, K., Kagami, M., Nagai, T., Kondoh, T., Onigata, K., Maeyama, K., Hasegawa, T., Hasegawa, Y., Yamazaki, T., Mizuno, S. *et al.* (2008) Molecular and clinical findings and their correlations in Silver-Russell syndrome: implications for a positive role of IGF2 in growth determination and differential imprinting regulation of the IGF2-H19 domain in bodies and placentas. *J. Mol. Med.*, **86**, 1171–1181.
21. Bruce, S., Hannula-Jouppi, K., Peltonen, J., Kere, J. and Lipsanen-Nyman, M. (2009) Clinically distinct epigenetic subgroups in Silver-Russell syndrome: the degree of H19 hypomethylation associates with SRS phenotype severity and genital and skeletal anomalies. *J. Clin. Endocrinol. Metab.*, **94**, 579–587.

22. Bartholdi, D., Krajewska-Walasek, M., Ounap, K., Gaspar, H., Chrzanowska, K.H., Ilyana, H., Kayserili, H., Lurie, I.W., Schinzel, A. and Baumer, A. (2009) Epigenetic mutations of the imprinted IGF2-H19 domain in Silver-Russell Syndrome (SRS): Results from a large cohort of patients with SRS and SRS-like phenotypes. *J. Med. Genet.*, **46**, 192–197.
23. Fedoriw, A.M., Stein, P., Svoboda, P., Schultz, R.M. and Bartolomei, M.S. (2004) Transgenic RNAi reveals essential function for CTCF in H19 gene imprinting. *Science*, **303**, 238–240.
24. Filippova, G.N., Qi, C.F., Ulmer, J.E., Moore, J.M., Ward, M.D., Hu, Y.J., Loukinov, D.I., Pugacheva, E.M., Klenova, E.M., Grundy, P.E. *et al.* (2002) Tumor-associated zinc finger mutations in the CTCF transcription factor selectively alter tts DNA-binding specificity. *Cancer Res.*, **62**, 48–52.
25. Schneid, H., Seurin, D., Vazquez, M.P., Gourmelen, M., Cabrol, S. and Le Bouc, Y. (1993) Parental allele specific methylation of the human insulin-like growth factor II gene and Beckwith-Wiedemann syndrome. *J. Med. Genet.*, **30**, 353–362.
26. Reik, W., Brown, K.W., Schneid, H., Le Bouc, Y., Bickmore, W. and Maher, E.R. (1995) Imprinting mutations in the Beckwith-Wiedemann syndrome suggested by altered imprinting pattern in the IGF2-H19 domain. *Hum. Mol. Genet.*, **4**, 2379–2385.
27. Scott, R.H., Douglas, J., Baskcomb, L., Huxter, N., Barker, K., Hanks, S., Craft, A., Gerrard, M., Kohler, J.A., Levitt, G.A. *et al.* (2008) Constitutional 11p15 abnormalities, including heritable imprinting center mutations, cause nonsyndromic Wilms tumor. *Nat. Genet.*, **40**, 1329–1334.
28. Renda, M., Baglivo, I., Burgess-Beusse, B., Esposito, S., Fattorusso, R., Felsenfeld, G. and Pedone, P.V. (2007) Critical DNA binding interactions of the insulator protein CTCF: a small number of zinc fingers mediate strong binding, and a single finger-DNA interaction controls binding at imprinted loci. *J. Biol. Chem.*, **282**, 33336–33345.
29. Lercher, M.J. and Hurst, L.D. (2003) Imprinted chromosomal regions of the human genome have unusually high recombination rates. *Genetics*, **165**, 1629–1632.
30. Sandovici, I., Kassovska-Bratinova, S., Vaughan, J.E., Stewart, R., Leppert, M. and Sapienza, C. (2006) Human imprinted chromosomal regions are historical hot-spots of recombination. *PLoS Genet.*, **2**, e101.
31. Hori, N., Nakano, H., Takeuchi, T., Kato, H., Hamaguchi, S., Oshimura, M. and Sato, K. (2002) A dyad oct-binding sequence functions as a maintenance sequence for the unmethylated state within the H19/Igf2-imprinted control region. *J. Biol. Chem.*, **277**, 27960–27967.
32. Kaufman, Y., Heled, M., Perk, J., Razin, A. and Shemer, R. (2009) Protein-binding elements establish in the oocyte the primary imprint of the Prader-Willi/Angelman syndromes domain. *Proc. Natl Acad. Sci. USA*, **106**, 10242–10247.
33. Zogel, C., Bohringer, S., Gross, S., Varon, R., Buiting, K. and Horsthemke, B. (2006) Identification of cis- and trans-acting factors possibly modifying the risk of epimutations on chromosome 15. *Eur. J. Hum. Genet.*, **14**, 752–758.
34. Donohoe, M.E., Silva, S.S., Pinter, S.F., Xu, N. and Lee, J.T. (2009) The pluripotency factor Oct4 interacts with Ctcf and also controls X-chromosome pairing and counting. *Nature*, **460**, 128–132.
35. Scott, R.H., Douglas, J., Baskcomb, L., Nygren, A.O., Birch, J.M., Cole, T.R., Cormier-Daire, V., Eastwood, D.M., Garcia-Minaur, S., Lupunzina, P. *et al.* (2008) Methylation-specific multiplex ligation-dependent probe amplification (MS-MLPA) robustly detects and distinguishes 11p15 abnormalities associated with overgrowth and growth retardation. *J. Med. Genet.*, **45**, 106–113.
36. Le Caignec, C., Gicquel, C., Gubler, M.C., Guyot, C., You, M.C., Laurent, A., Joubert, M., Winer, N., David, A. and Rival, J.M. (2004) Sonographic findings in Beckwith-Wiedemann syndrome related to H19 hypermethylation. *Prenat. Diagn.*, **24**, 165–168.
37. Takai, D., Gonzales, F.A., Tsai, Y.C., Thayer, M.J. and Jones, P.A. (2001) Large scale mapping of methylcytosines in CTCF-binding sites in the human H19 promoter and aberrant hypomethylation in human bladder cancer. *Hum. Mol. Genet.*, **10**, 2619–2626.
38. Ulaner, G.A., Yang, Y., Hu, J.F., Li, T., Vu, T.H. and Hoffman, A.R. (2003) CTCF binding at the insulin-like growth factor-II (IGF2)/H19 imprinting control region is insufficient to regulate IGF2/H19 expression in human tissues. *Endocrinology*, **144**, 4420–4426.
39. Gicquel, C., Raffin-Sanson, M.L., Gaston, V., Bertagna, X., Plouin, P.F., Schlumberger, M., Louvel, A., Luton, J.P. and Le Bouc, Y. (1997) Structural and functional abnormalities at 11p15 are associated with the malignant phenotype in sporadic adrenocortical tumors: study on a series of 82 tumors. *J. Clin. Endocrinol. Metab.*, **82**, 2559–2565.
40. Cui, H., Niemitz, E.L., Ravenel, J.D., Onyango, P., Brandenburg, S.A., Lobanenkov, V.V. and Feinberg, A.P. (2001) Loss of imprinting of insulin-like growth factor-II in Wilms' tumor commonly involves altered methylation but not mutations of CTCF or its binding site. *Cancer Res.*, **61**, 4947–4950.
41. Yeh, A., Wei, M., Golub, S.B., Yamashiro, D.J., Murty, V.V. and Tycko, B. (2002) Chromosome arm 16q in Wilms tumors: unbalanced chromosomal translocations, loss of heterozygosity, and assessment of the CTCF gene. *Genes Chromosomes Cancer*, **35**, 156–163.